RSC Advances

ROYAL SOCIETY OF CHEMISTRY

www.rsc.org/advances

RSC Advances

ARTICLE

Determination of DNA Adenine Methylation in Genomes of Mammals and Plants by Liquid Chromatography / Mass Spectrometry

Received 00th January 2015,
Accepted 00th January 2015

DOI: 10.1039/x0xx00000x

www.rsc.org/

Wei Huang,[1] Jun Xiong,[1] Ying Yang,[2] Song-Mei Liu,[2] Bi-Feng Yuan,[1,*] ,Yu-Qi Feng[1]

DNA adenine methylation (N^6-methyl-2'-deoxyadenosine, m^6dA) plays important functional roles in prokaryotes and protist, including regulation of gene transcription, DNA replication and repair, and the restriction-modification system. Whereas, there is no definitive evidence supporting for the presence of DNA adenine methylation in genomic DNA of higher eukaryotes, such as mammals and plants, where DNA cytosine methylation (5-methylcytosine) instead is well recognized as an important epigenetic mark that has regulatory roles in various biological processes. In the current study, we developed a Dpn I cleavage coupled with size-exclusion ultrafiltration method, with which we discovered the wide-spread existence of m^6dA in genomic DNA of higher eukaryotes, including human cells, rat tissues, and plants besides bacteria and protist by employing high-resolution mass spectrometry analysis. And the contents of m^6dA vary in different cell types with the range of 0.00006 to 0.00077% (m^6dA/dA). Moreover, similar to N^6-methyladenosine (m^6A) in RNA, m^6dA contents significantly decreased in type 2 diabetes mellitus (T2DM) patients compared to control subjects, indicating m^6dA plays important roles in the pathogenesis of T2DM as m^6A. In addition, knockdown of cellular fat mass and obesity-associated (FTO) protein increased the m^6dA content, while overexpression of cellular FTO decreased m^6dA content in DNA, suggesting m^6dA and m^6A may share the same demethylase of FTO. The demonstration of the universal presence of DNA adenine methylation constitutes the first and essential step toward understanding of m^6dA functions in higher eukaryotes.

Introduction

Accumulating evidence suggests that DNA adenine methylation (N^6-methyl-2'-deoxyadenosine, m^6dA) plays various functional roles in prokaryotes.[1] DNA adenine methylation is related to the host-specific restriction-modification (R-M) system. The R-M system is taken as a defense mechanism against bacteriophage infection in bacteria, in which methylation of bacterial DNA protects it from the action of the corresponding restriction endonuclease digestion; whereas unmethylated sites of foreign DNA such as bacteriophage DNA are cleaved.[2, 3] In addition, DNA adenine methylation can regulate gene transcription through modulating the binding of regulatory proteins to DNA.[4, 5] Moreover, DNA adenine methylation was found to be required for the control of initiation of DNA replication[6, 7] and was involved in DNA mismatch repair.[8]

In addition to the wide existence in prokaryotes, DNA adenine methylation has also been found to be present in DNA of several protist, including genera Chlamydomonas, Chlorella, Oxytricha, Paramecium and Tetrahymena.[9-11] One previous study also reported the existence of m^6dA in DNA of human, *Drosophila* and mealybug by immunochemical method;[12] however, the result is not conclusive since the possible contamination of RNA and the less specify of used antibodies. To the best of our knowledge, there is no other definitive evidence supporting for the presence of DNA adenine methylation in genomic DNA of higher eukaryotes, such as mammals and plants. During the revision of this manuscript, three papers have been published for the discovery of m^6dA in eukaryotes, indicating that m^6dA may serve as novel potential epigenetic mark.[13-15] Instead, DNA cytosine methylation (5-methylcytosine, 5-mC) in genomic DNA of mammals and plants is well recognized as an important

[1] Key Laboratory of Analytical Chemistry for Biology and Medicine (Ministry of Education), Department of Chemistry, Wuhan University, Wuhan 430072, P.R. China
[2] Center for Gene Diagnosis, Zhongnan Hospital of Wuhan University, Donghu Road 169#, Wuhan, 430071, P.R. China
*To whom correspondence should be addressed. Tel.:+86-27-68755595; fax: +86-27-68755595. E-mail address: bfyuan@whu.edu.cn
† Electronic Supplementary Information (ESI) available: See DOI: 10.1039/x0xx00000x

epigenetic mark that has regulatory roles in various biological processes.[16-19] Properly established and maintained DNA cytosine methylation patterns are crucial for the normal functions of living cells.[20]

The assumption that DNA adenine methylation does not occur in mammals and plants is based on the use of low-sensitivity methods with a detection limit of 0.01-0.1% (m^6dA/dA), including radioactive labeling method, HPLC-UV method, and micellar electrokinetic chromatography-laser-induced fluorescence method.[21-23] The sensitivity may not be enough to discover m^6dA in DNA if it occurs in a rare population in higher eukaryotes. Nevertheless, it should be pointed out that an overall content of modified nucleosides less than 0.0001% may be biologically significant if it occurs in specific gene regulatory elements, such as recently discovered 5-hydroxymethtylcytosine (5-hmC).[24, 25] Hence, according to the size of the human genome (~ 3×10^9 bp), the presence of a few hundred m^6dA may be sufficient to play a crucial role in the regulation of biological processes, which points to the importance of highly specific and sensitive methods to investigate the presence of m^6dA in DNA of higher eukaryotes. In addition, the essential roles of DNA adenine methyltransferases in bacterial viability and virulence underscore the importance for the investigation of the presence and biological functions of DNA adenine methylation in higher eukaryotes. Therefore, the knowledge of the DNA adenine methylation status in eukaryotic DNA is necessary for development of antibiotics targeting bacterial DNA adenine methyltransferases.

Unlike DNA adenine methylation, RNA adenine methylation (N^6-methyladenosine, m^6A) has long been identified to exist in both prokaryotes and eukaryotes with high abundance.[26-28] The cell-type and cell-state-dependent m^6A distribution indicates that m^6A modifications are highly dynamic.[29, 30] Recent studies have also demonstrated that m^6A plays critical roles in DNA transcription, RNA stability, translational regulation and microRNA maturation, and thus involves in a variety of biological processes including adipogenesis, spermatogenesis, development, carcinogenesis, circadian rhythm and stem cell renewal.[31-34] Considering 5-methylcytosine that is widely viewed as the fifth base in genomic DNA exists in both DNA (5-methyl-2'-deoxycytidine) and RNA (5-methylcytidine), we hypothesize that m^6dA may also occur in DNA as m^6A in RNA in higher eukaryotes (Figure 1).With respect to the essential roles of m^6dA in DNA in prokaryotes and protist and the wide existence of m^6A in RNA of higher eukaryotes, here we explored m^6dA modification in DNA of higher eukaryotes by employing high-resolution mass spectrometry analysis. Our results demonstrated that m^6dA is widely present in higher eukaryotes, including mammals and plants. And m^6dA contents vary largely in different cell lines and tissues. In our previous study, we demonstrated the m^6A contents in peripheral blood RNA from type 2 diabetes mellitus (T2DM) patients were significantly lower compared to the healthy controls.[35] Here we further discovered that m^6dA from peripheral blood DNA also significantly decreased in T2DM patients compared to the healthy controls. In addition, knockdown and overexpression of cellular fat mass and obesity-associated protein (FTO) changed m^6dA contents in DNA and m^6A contents in RNA, suggesting both m^6dA and m^6A may share the same demethylase of FTO.

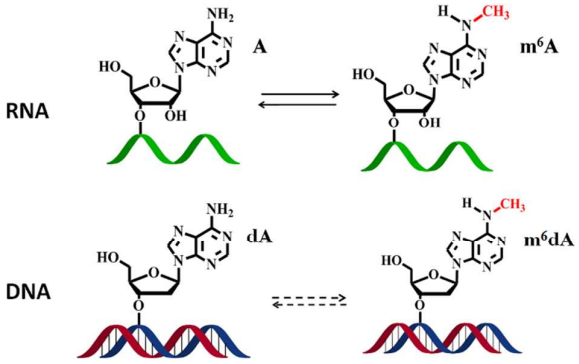

Figure 1. RNA adenine methylation and DNA adenine methylation.

Experimental

Chemicals and reagents

2'-deoxycytidine (dC), 2'-deoxyguanosine (dG), 2'-deoxyadenosine (dA), thymidine (T), cytidine (rC), guanosine (rG), adenosine (rA), uridine (rU) were purchased from Sigma-Aldrich (Beijing, China). N^6-methyl-deoxyadenosine (m^6dA) was obtained from Berry & Associates Inc. (Michigan, USA). N^6-methyladenosine (m^6A) was from Hanhong Chemical Co., Ltd. (Shanghai, China). S1 nuclease and calf intestinal alkaline phosphatase (CIAP) were from Takara Biotechnology (Dalian, China). Phosphodiesterase I was purchased from Sigma-Aldrich (St. Louis, MO, USA). Chromatographic grade methanol was purchased from Merck (Darmstadt, Germany). Agarose, tris hydroxy methyl aminomethan (Tris), ethylene diamine tetraacetic acid (EDTA), boric acid, chloroform and formic acid (FA) were purchased from Sinopharm Chemical Reagent Co., Ltd. (Shanghai, China). The water used throughout the study was purified by a Milli-Q apparatus (Millipore, Bedford, MA). Stock solutions of these nucleosides were prepared in Milli-Q water at a concentration of 4 mmol/L.

Biological samples and DNA extraction

Human leukemia Jurkat T cells (Jurkat-T), human embryonic kidney cells (293T), GW5100 *E. coli* cells were obtained from the Cell Bank of Type Culture Collection, Chinese Academy of Sciences, and cultured according to previously described method.[36, 37] Ciprofloxacin (10 μg/ml) was added in the culture medium to inhibit the possible contamination of *Mycoplasma*. Genomic DNA was

extracted using DNAiso Reagent (Takara Biotechnology, Dalian, China) according to the manufacture recommended procedure.

Male Sprague-Dawley rat (4 weeks old) was obtained from the Center for Animal Experiment/ABSL-3 Laboratory of Wuhan University and sacrificed to collect tissues and stored under -80 °C. Genomic DNA was extracted using E.Z.N.A.® Tissue DNA kit (Omega Bio-Tek Inc., Norcross, GA, USA) according to the manufacture recommended procedure.

Plant samples, including *Oryza sativa* and *Zea mays* were used in this study. The culturing conditions were according to our previously reported method.[38] Plant genomic DNA was isolated using E.Z.N.A.® plant DNA kit (Omega Bio-Tek Inc., Norcross, GA, USA) according to the manufacture recommended procedure.

Fresh peripheral blood samples of 15 T2DM patients and 15 participants randomly selected from healthy individuals who had no history of endocrine disease or chronic disease were stored at 4 °C in the presence of EDTA as an anticoagulant. An aliquot of 500 μL of blood was subjected to extraction of DNA using the E.Z.N.A.® blood DNA kit (Omega Bio-Tek Inc., Norcross, GA, USA) following the manufacture recommended procedure. Written informed consent was obtained from all subjects. This study was approved by the ethics committee of Zhongnan Hospital of Wuhan University and conducted in accordance with the Helsinki Declaration.

Knockdown and overexpression of *FTO* by transfection

FTO siRNA were synthesized by Takara Biotechnology (Dalian, China). The target FTO mRNA sequence is 5'-AAAUAGCCGCUGCUUGUGAGA-3' according to previous report.[39] A non-sense siRNA with the sequence 5'-UUCUCCGAACGUGUCACGUTT-3' was used as the control. For the overexpression of *FTO*, we constructed a vector pcDNA3.1-FTO, and the empty vector pcDNA3.1 was served as the control. Lipofectamine RNAiMAX (Invitrogen) and Lipofectamine 2000 (Invitrogen) were used to perform siRNA and plasmid transfection, respectively, according to the manufacturer's instructions. The mRNA expression level of *FTO* after knockdown and overexpression was determined by quantitative real-time PCR (CFX96 Touch™, BIORAD) according to our previously described method[35].

Enzymatic digestion of DNA

The extracted genomic DNA was first digested by Dpn I restriction enzyme followed by ultrafiltration to remove the possible contamination of bacterial DNA (Figure 2). Typically, a 50-μL mixture including 6 ug genomic DNA, 5 μL 10× cutsmart buffer (New England Biolabs, Ipswich, WA), 80 units of Dpn I restriction enzyme (4 μL, New England Biolabs, Ipswich, WA) and 41 μL H_2O was incubated at 37 °C for 2 h. Then the reaction solution was transferred to a 100 kD cut-off centrifugal filter (Millipore, Bedford, MA) and centrifuged at 8000×*g* for 3 min. The centrifugal filter was washed 10 times with 200 μL of water for each time. The DNA retained on the filter was then desorbed by water.

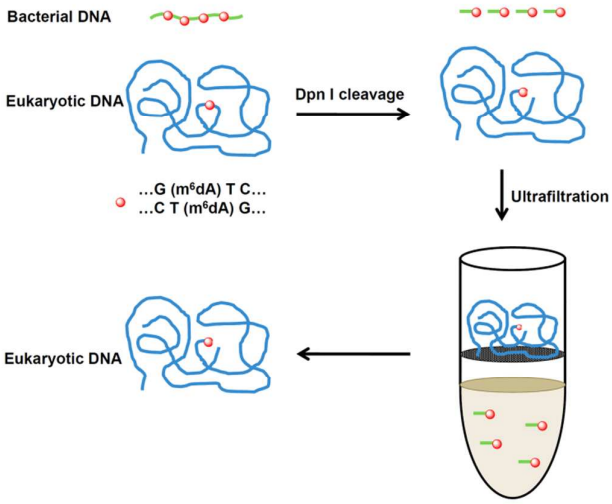

Figure 2. Schematic diagram for the elimination of possible contamination of bacterial DNA by Dpn I cleavage coupled with size-exclusion ultrafiltration.

The resulting genomic DNA was enzymatically digested according to previously described method.[40] Briefly, genomic DNA (5 μg in 16 μL H_2O) was first denatured by heating at 95 °C for 5 min and then chilling on ice for 2 min. After adding 2 μL of S1 nuclease buffer (30 mM CH_3COONa, pH 4.6, 280 mM NaCl, 1 mM $ZnSO_4$) and 360 units of S1 nuclease (2 μL), the mixture (20 μL) was then incubated at 37 °C for 16 h. To the solution was subsequently added 10 μL of alkaline phosphatase buffer (50 mM Tris-HCl, 10 mM $MgCl_2$, pH 9.0), 0.005 units of venom phosphodiesterase I (5 μL), 30 units of alkaline phosphatase (1 μL) and 64 μL H_2O. And then the incubation was continued at 37 °C for an additional 4 h followed by extraction with equal volume of chloroform twice. The resulting aqueous layer was collected and lyophilized to dryness and then reconstituted in 100 μL water followed by analysis with liquid chromatography-electrospray ionization-tandem mass spectrometry (LC-ESI-MS/MS) analysis.

LC-ESI-MS/MS analysis

Analysis of the mammals and plants samples was performed on LC-ESI-MS/MS system consisting of an AB 3200 QTRAP mass spectrometer (Applied Biosystems, Foster City, CA, USA) with an electrospray ionization source (Turbo Ionspray) and a Shimadzu LC-20AD HPLC (Tokyo, Japan) with two LC-20AD pumps, a SIL-20A autosampler, a CTO-20AC thermostatted column compartment, and a DGU-20A3 degasser. Data acquisition and processing were performed using AB SCIEX Analyst 1.5 Software (Applied Biosystems, Foster City, CA). The HPLC separation was performed on a Hisep C18-T column

(150 mm×2.1 mm i.d., 5 μm, Weltech Co., Ltd., Wuhan, China) with a flow rate of 0.2 mL/min at 35 °C. FA in water (0.1%, v/v, solvent A) and FA in methanol (0.1% v/v, solvent B) were employed as mobile phase. A gradient of 5 min 5% B, 10 min 5% -30% B, 5 min 30% -50% B, 3 min 50% -5% B and 17 min 5% B was used.

The mass spectrometry detection was performed under positive electrospray ionization mode. The target nucleosides were monitored by multiple reaction monitoring (MRM) mode using the mass transitions (precursor ions → product ions) of dC (228.4 → 112.2), T (243.3 → 127.2), dA (252.4 → 136.2), dG (268.4 → 152.4), m^{6}dA (266.1 →150.2), rC (244.4 → 112.2), rU (245.4 → 113.1), rA (268.4 → 136.2), rG (284.5 → 152.2), m^{6}A (282.2 →150.1). The MRM parameters of all nucleosides were optimized to achieve maximal detection sensitivity (Table S1, Supporting Information).

Investigation of the retention behavior of m^{6}dA

To confirm m^{6}dA in genomic DNA of higher eukaryotes, the retention behavior of suspected m^{6}dA from genomic DNA of 293T cells was compared with m^{6}dA standard using different columns. Besides the reversed-phase Hisep C18-T column, Hisep OTS column (mix-mode C8-SO_3, 150 mm×2.1 mm i.d., 5 μm, Weltech Co., Ltd., Wuhan, China) and HILIC pNA-sil column (150 mm×2.1 mm i.d., 5 μm) [41] were also used. As for the Hisep OTS column, solvent A (2.5 mM $HCOONH_4$ and 0.01% FA in H_2O) and solvent B (2.5 mM $HCOONH_4$ and 0.01% FA in CH_3OH) were used as mobile phase. A gradient of 9 min 3% -13% B, 1 min 13% -40% B, 20 min 40% -80% B, 2 min 80% B, 2 min 80% -3% B, 10 min 3% B was used. As for the HILIC pNA-sil column, H_2O/ACN (15/85, v/v) containing 0.01% FA was used as mobile phase for isocratic elution. A flow rate of 0.2 mL/min at 35 °C was used for both columns.

Determination of m^{6}dA by high-resolution mass spectrometry

High-resolution mass spectrometry analysis was performed using LTQ XL Orbitrap mass spectrometer (Thermo Fisher Scientific). The HPLC separation was performed on a Zorbax SB-C18 column (2.1 mm×150 mm, 5 μm, Agilent). Methanol/water was used as mobile phase with the flow rate of 0.2 mL/min, which was delivered using an Agilent 1100 HPLC pump. A gradient of 2 min 5% methanol, 8 min 5%-100% methanol, 5 min 100%-5% methanol and 7 min 5% methanol was employed for the separation. A full MS scan and a MS/MS scan were used to elucidate the structural information of m^{6}dA.

Calculation of the percentage of DNA and RNA adenine methylation

m^{6}dA content in DNA and m^{6}A content in RNA were calculated using the following expression:

$$\text{m}^6\text{dA (or m}^6\text{A) \%} = \frac{\text{M}_{\text{m}^6\text{dA (or m}^6\text{A)}}}{\text{M}_{\text{dA (or rA)}}} \times 100\%$$

where $M_{m^6dA\ (or\ m^6A)}$ is the molar quantity of m^{6}dA or m^{6}A, and $M_{dA\ (or\ rA)}$ is the molar quantity of dA or rA determined in DNA or RNA sample.

Statistical analysis

Statistical analyses were performed using SPSS 19.0 software (SPSS Inc., Chicago, USA). Student's unpaired t-test was used to assess the differences of DNA and RNA adenine methylation. All p values were two-sided, and $p <$ 0.05 were considered to be statistically significant.

Results and discussion

The fundamental role of m^{6}dA in bacteria raises fascinating questions on its phyletic distribution and possible existence in higher mammals and plants. Previous reports suggested no detectable m^{6}dA was observed in DNA of mammals or plants, which, however, could be due to the less sensitive detection methods used as well as the low abundance of m^{6}dA in DNA of higher eukaryotes [1]. It is worth noting that an overall content even less than 0.0001% of modified nucleosides in DNA can be biologically significant. Therefore, it is necessary to reinvestigate the existence of m^{6}dA in genomic DNA of higher eukaryotes with highly sensitive detection method.

Discovery of m^{6}dA in genomic DNA of mammalian cells by LC-ESI-MS/MS

Here we developed a sensitive LC-ESI-MS/MS method to explore m^{6}dA modification in DNA of mammals and plants. In this respect, we monitored m^{6}dA from the sample of digested genomic DNA of 293T cells by LC-ESI-MS/MS under MRM mode. The result showed a suspected peak that had a similar retention time as m^{6}dA standard was observed (Figure 3), suggesting the possible existence of m^{6}dA in genomic DNA of 293T cells.

Because m^{6}dA modification that exists in genomic DNA of bacteria may contaminate cultured eukaryotic cells and tissues, elimination of bacterial contamination is therefore essential to avoid the false positive result. To this end, taken the advantage of Dpn I selective cleavage of G(m^{6}dA)TC sites in DNA,[42, 43] bacterial DNA can be cut into short fragments since adenines in bacteria DNA are heavily modified to m^{6}dA. And only the methylated adenine (m^{6}dA) in the recognition sites will be cleaved by Dpn I, while normal adenine in GATC sites cannot be degraded. On the other side, due to the extremely low abundance of m^{6}dA in genomic DNA of mammals and plants, the DNA of mammals and plants remains in large-size after Dpn I digestion. Therefore, the small DNA fragments of bacteria can be subsequently removed from large-size genomic DNA of mammals and plants using size-exclusion ultrafiltration (Figure 2). In this respect, the agarose gel electrophoresis results showed that after Dpn I digestion, most of the fragments of bacterial DNA are smaller than 2500 bp (Figure 4, lane 3), suggesting efficient cleavage of bacterial DNA. While no obvious

change of genomic DNA of 293T cells was observed after Dpn I digestion (Figure 4, lane 4 and lane 5), which is due to the relatively low abundance of m^{6}dA existing in large-size genomic DNA of mammals and plants. These results indicated that Dpn I could efficiently cleave bacterial DNA but not eukaryotic DNA.

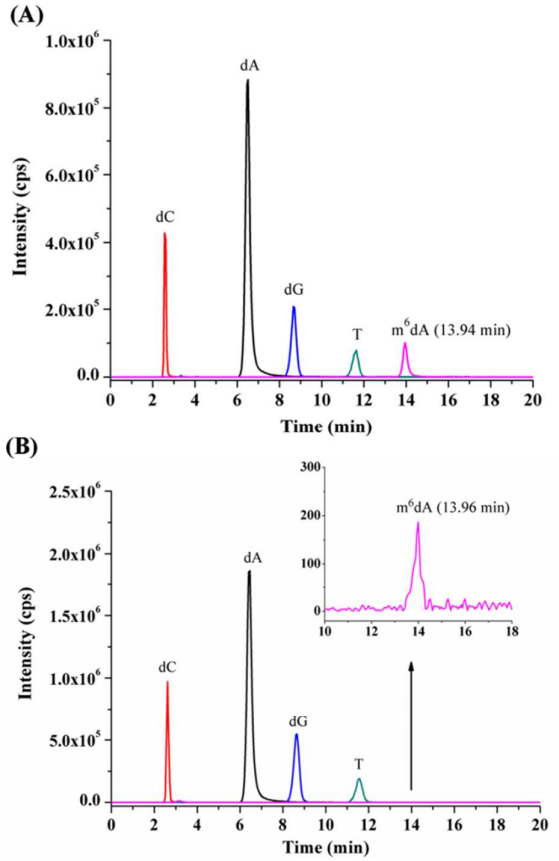

Figure 3. The MRM chromatograms of nucleosides. (A) Standard nucleosides. (B) Genomic DNA from 293T cells after enzymatic digestion. Shown in inset is the enlargement chromatogram of m^{6}dA. Separation column, reversed-phase Hisep C18-T column.

Then after Dpn I digestion, the small bacterial DNA fragments could be efficiently removed by size exclusion ultrafiltration, while the large-size eukaryotic DNA retained on the filter. As shown in Figure S1A and S1B, m^{6}dA is undetectable after Dpn I digestion and size-exclusion ultrafiltration even using 100 ng bacterial DNA. In addition, the signal of m^{6}dA in 5 μg genomic DNA of 293T cells (Figure S1C, Supporting Information) is much lower than that of 100 ng bacterial DNA (Figure S1A, Supporting Information). Therefore, the bacterial DNA contamination in 293T cells should be less than 100 ng if 293T cells were contaminated by bacteria. Because 100 ng bacterial DNA can be efficiently removed (comparing Figure S1A and S1B, Supporting Information), the Dpn I cleavage coupled with size-exclusion ultrafiltration method demonstrated to be capable to effectively eliminate bacterial DNA contamination in the determination of m^{6}dA in eukaryotic cells. And therefore the signal observed in 293T cells after Dpn I cleavage coupled with size-exclusion ultrafiltration treatment should be from the genomic DNA of 293T cells (Figure S1D, Supporting Information). Therefore, all the following DNA samples were treated with Dpn I cleavage coupled with size-exclusion ultrafiltration to eliminate possible bacterial DNA contamination.

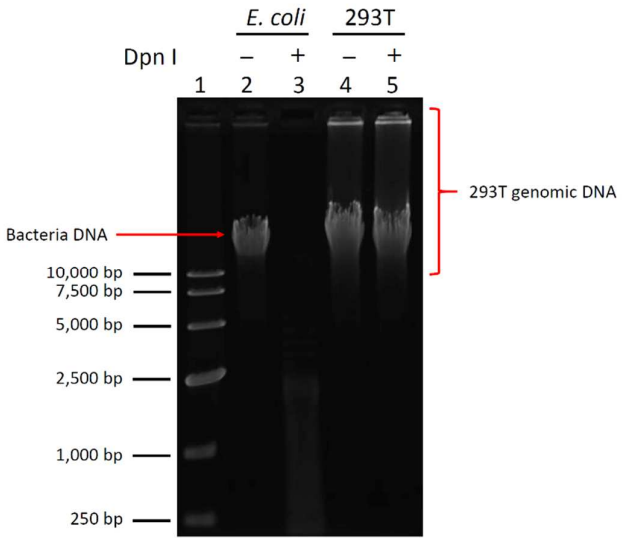

Figure 4. Agarose gel electrophoresis analysis of DNA samples digested by Dpn I restriction enzyme. After Dpn I restriction enzyme cleavage, the DNA samples were loaded into a 0.8% agarose gel for electrophoresis with 0.5×TBE at 120 V for 1 h at room temperature. The gel was then staining by GelRed (Biotium, Inc., USA) and analysed using the Pharos FX Molecular Imager (Bio-Rad, USA). Lane 1, DNA marker; Lane 2, bacterial DNA; Lane 3, bacterial DNA digested by Dpn I; Lane 4, 293T genomic DNA; Lane 5, 293T genomic DNA digested by Dpn I.

RSC Advances

ARTICLE

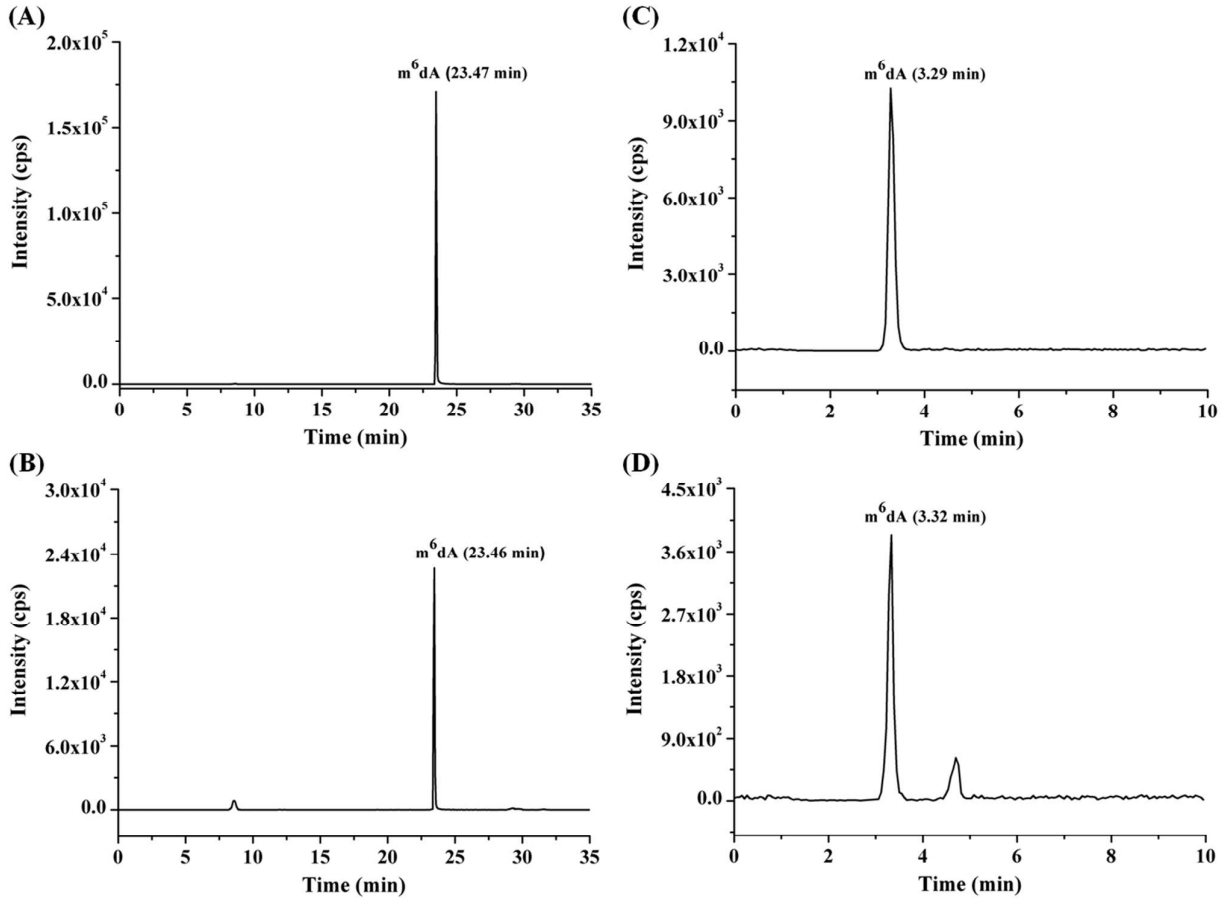

Figure 5. Retention of the m^{6}dA on different separation columns. (A) MRM chromatogram of m^{6}dA standard on mix-mode C8-SO_3 column. (B) MRM chromatogram of putative m^{6}dA in genomic DNA of 293T cells on mix-mode C8-SO_3 column. (C) MRM chromatogram of m^{6}dA standard on HILIC pNA-sil column. (D) MRM chromatogram of putative m^{6}dA in genomic DNA of 293T cells on HILIC pNA-sil column.

To further confirm the identity of the observed peak, we compared the retention time of m^{6}dA standard and the suspected m^{6}dA from genomic DNA of 293T cells using different columns in the LC-ESI-MS/MS analysis. In this respect, a Hisep OTS column and a HILIC pNA-sil column were used besides the reversed-phase C18 column. The retention time on Hisep OTS column was 23.47 min for m^{6}dA standard (Figure 5A) and 23.46 min for the suspected m^{6}dA peak from genomic DNA of 293T cells (Figure 5B). Likewise, the retention time on HILIC pNA-sil column was 3.29 min for m^{6}dA standard (Figure 5C) and 3.32 min for the suspected m^{6}dA peak from genomic DNA of 293T cells (Figure 5D). The high consensus on retention times of m^{6}dA standard and the suspected m^{6}dA peak from genomic DNA of 293T cells under different HPLC separation mode revealed that these two peaks could represent the same compound.

Validation of m^{6}dA in genomic DNA of higher eukaryotes by high-resolution mass spectrometry analysis

We further compared the fragmentation pattern of the m^{6}dA standard and the putative m^{6}dA in genomic DNA of 293T cells using high-resolution LTQ XL Orbitrap mass spectrometer. The results showed that two ions of *m/z* 266.1243 and *m/z* 150.2387, which represent the parent ion of m^{6}dA and its product ion, were observed for m^{6}dA standard under full scan mode (Figure 6A). As expected, two ions of *m/z* 266.1237 and *m/z* 150.2392 were

observed for the putative m⁶dA in genomic DNA of 293T cells under full scan mode (Figure 6B). And further fragmentation of m⁶dA base ion was conducted. The results showed that fragmentation patterns of m⁶dA standard and putative m⁶dA in genomic DNA of 293T cells were identical (Figure 6C and 6D), which further confirmed the existence of m⁶dA in genomic DNA of 293T cells.

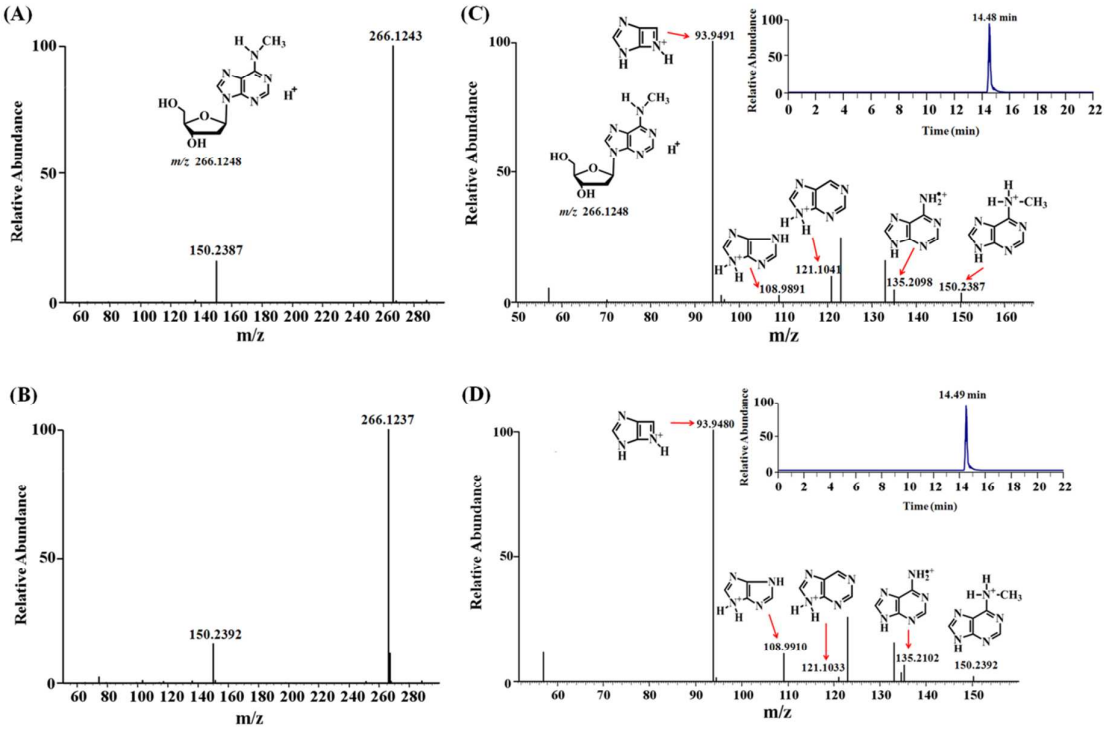

Figure 6. Analysis of m⁶dA by high-resolution mass spectrometry. (A) Full scan spectrum of m⁶dA standard. (B) Full scan spectrum of putative m⁶dA in genomic DNA of 293T cells. (C) Product ion spectrum of m⁶dA standard. (D) Product ion spectrum of putative m⁶dA in genomic DNA of 293T cells.

Widespread existence of m⁶dA in genomic DNA of higher eukaryotes

To quantify the content of m⁶dA in genomic DNA of higher eukaryotes, we first made the calibration curve, which was constructed by plotting the mean peak area ratio of m⁶dA/dA versus the mean molar ratio of m⁶dA/dA based on data obtained from triplicate measurements. The results showed that good linearities within the range of 0.00005-0.002% and 0.002-0.5% of m⁶dA/dA were obtained with correlation coefficients (R) being greater than 0.99 (Table 1). Limit of detection (LOD) and limit of quantification (LOQ) for m⁶dA were calculated as the amounts of the analyte at Signal/Noise ratios of 3 and 10, respectively. The LOD and LOQ were 0.42 fmol and 1.38 fmol for m⁶dA, respectively (Table 1), with which as low as 0.00001% m⁶dA (m⁶dA/dA) can be determined using 5 μg genomic DNA.

Table 1. Linearity, LOD and LOQ of m⁶dA by LC-ESI-MS/MS analysis.

Linear range (m⁶dA/dA, %)	Regression line		R^2	LOD (fmol)	LOQ (fmol)
	Slope	Intercept			
0.00005-0.002	0.1506	0.000087	0.9983	0.42	1.38
0.002-0.5	0.1271	0.000134	0.9997		

We then further quantified m⁶dA in genomic DNA of various higher eukaryotes, including 2 human cell lines, 7 rat tissues and 2 kinds of plants. After Dpn I cleavage, ultrafiltration, and enzymatic digestion, the resulting nucleosides were subjected to LC-ESI-MS/MS analysis. Our results showed that m⁶dA can be detected in all the examined samples with m⁶dA contents ranging from 0.00006 to 0.00077% (m⁶dA/dA) (Table 2). Shown in Figure 7 are the typical MRM chromatograms of nucleosides of 293T cells, rat heart tissue and *Oryza sativa* leaves. These results demonstrated that m⁶dA widely exists in higher eukaryotes, which constituted the first and essential step toward understanding the

functions of DNA adenine methylation in higher eukaryotes.

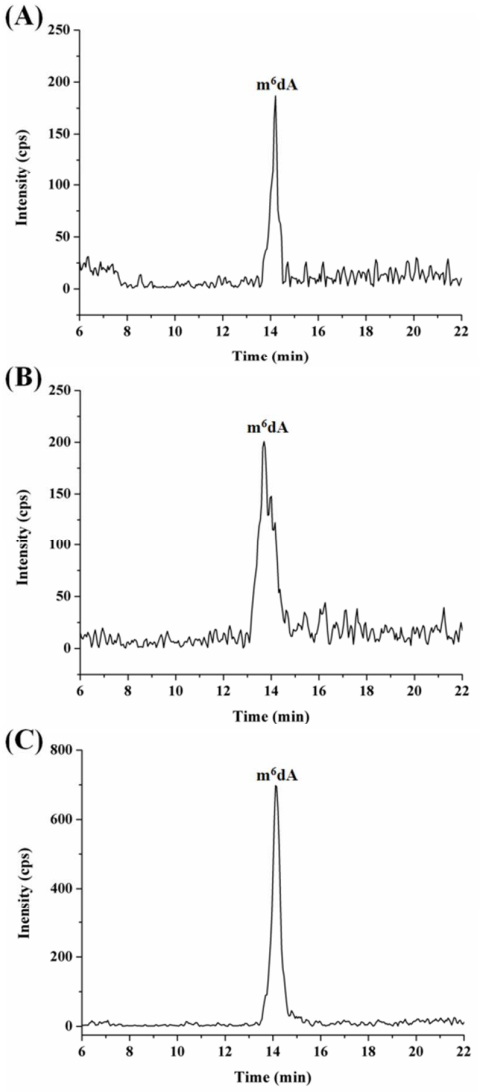

Figure 7. Typical MRM chromatograms for determination of m⁶dA in genomic DNA of mammals and plants. (A) 293T cells. (B) Rat heart tissue. (C) *Oryza sativa* leaves.

Table 2. m⁶dA contents in genomic DNA of mammals and plants.

	Sample name	m⁶dA/dA, %
Human cells	293T	0.00017 ± 0.00001
	Jurkat-T	0.00023 ± 0.000001
Rat tissues	Heart	0.00032 ± 0.00003
	Liver	0.00013 ± 0.00001
	Spleen	0.00009 ± 0.00001
	Lung	0.00008 ± 0.000003
	Kidney	0.00006 ± 0.00001
	Brain	0.00013 ± 0.00002
	Subcutis	0.00013 ± 0.00002
Plants	Leaves of Oryza sativa	0.00077 ± 0.000004
	Kernels of Zea mays	0.00015 ± 0.00003

m⁶dA contents decreased in genomic DNA of diabetic patients

Previously Jia et al. reported that the methyl group of m⁶A in RNA can be enzymatically removed by FTO protein.[39] In addition, they found that FTO protein also can remove the methyl group of m⁶dA in synthetic DNA, indicating m⁶A and m⁶dA may share the same demethylase of FTO due to their similar chemical structure. On the other side, our recent study demonstrated that m⁶A contents in RNA from the peripheral blood cells of type 2 diabetes mellitus (T2DM) patients were significantly lower compared to the healthy controls and T2DM can be characterized by the content of m⁶A.[35] The decreased m⁶A in T2DM patients resulted from the significantly increased expression of FTO that is responsible for the demethylation of m⁶A. In this respect, since the m⁶A demethylase of FTO could also function on m⁶dA in synthetic DNA,[39] we hypothesize that m⁶dA contents in DNA from the peripheral blood cells of T2DM patients may also decrease like m⁶A in RNA compared to the healthy controls.

In this respect, we then analyzed m⁶A and m⁶dA contents in RNA and DNA, respectively, from 15 T2DM patients and 15 control subjects by LC-ESI-MS/MS (Table S2 in Supporting Information). The mean content of m⁶A in RNA of T2DM patients (0.12 ± 0.02 %) is significantly lower compared to the controls (0.18 ± 0.04 %, p = 8.9×10^{-7}) (Figure 8A), which is consistent with our previous study [35]. As expected, the mean content of m⁶dA in DNA of T2DM patients (0.00028 ± 0.00003%) is also significantly lower compared to the controls (0.00033 ± 0.00006%, p = 0.004) (Figure 8B), indicating that the decrease of both m⁶A and m⁶dA could be due to the increased level of FTO in T2DM patients.

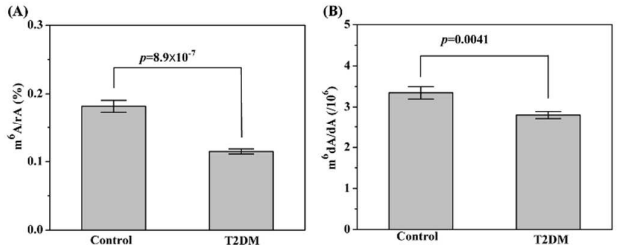

Figure 8. Quantification and statistical analysis of RNA adenine methylation and DNA adenine methylation in T2DM patients (n=15) and control subjects (n=15). (A) The average contents of m⁶A in RNA of T2DM patients and control subjects. (B) The average contents of m⁶dA in DNA of T2DM patients and control subjects.

m⁶dA contents change in *FTO* knockdown and overexpression cell line

Here we also evaluated the m⁶dA contents change in *FTO* knockdown as well as overexpression cell line. The RT-qPCR results showed that *FTO* expression levels were significantly lower in FTO knockdown cells and significantly higher in FTO overexpression cells (Figure S2). As expected, the results showed m⁶dA contents

increased in *FTO* knockdown cell line and decreased in *FTO* overexpression cell line (Figure 9A). In addition, m^{6}A from RNA also exhibited the similar trend of contents change as that of m^{6}dA (Figure 9B). The results further suggested that m^{6}dA and m^{6}A may share the same demethylase of FTO. On the other side, the m^{6}dA contents change induced by *FTO* knockdown and overexpression further supported the real existence of m^{6}dA in genomic DNA of mammalian cells because m^{6}dA contents will not change with *FTO* knockdown or overexpression if m^{6}dA is from bacterial DNA.

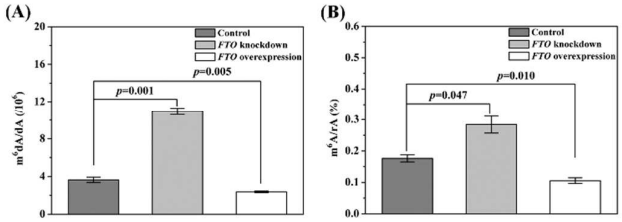

Figure 9. FTO regulates m^{6}dA and m^{6}A contents in DNA and RNA, respectively. (A) m^{6}dA contents change upon *FTO* gene knockdown and overexpression. (B) m^{6}A contents change upon *FTO* gene knockdown and overexpression.

Conclusion

Like DNA cytosine methylation (5-mC) that has long been recognized as an important epigenetic modification in genomes, DNA adenine methylation (m^{6}dA) may also play critical regulatory roles in cellular processes. By developing a Dpn I cleavage coupled with size-exclusion ultrafiltration method, we were able to efficiently eliminate the possible bacterial DNA contamination in eukaryotic DNA. Using the developed Dpn I cleavage coupled with size-exclusion ultrafiltration method and high-resolution mass spectrometry analysis, we demonstrated the universal presence of DNA adenine methylation in higher eukaryotes in the current study, which constitutes the first and essential step toward understanding the functions of DNA adenine methylation in higher eukaryotes. In future study, the genome-wide localization analysis of DNA adenine methylation could offer new insight on their functions in cellular and pathological processes.

Acknowledgements

The authors thank the financial support from the National Basic Research Program of China (973 Program) (2012CB720601) and the National Natural Science Foundation of China (21205091, 81271919, 81472023). And we thank Dr Hao-Yang Wang (Shanghai Institute of Organic Chemistry, Chinese Academy of Sciences) for the help on the interpretation of the high-resolution mass spectrometry of m^{6}dA.

References

1. D. Ratel, J. L. Ravanat, F. Berger and D. Wion, *Bioessays*, 2006, 28, 309-315.
2. G. Bertani and J. J. Weigle, *Journal of bacteriology*, 1953, 65, 113-121.
3. S. E. Luria and M. L. Human, *J Bacteriol*, 1952, 64, 557-569.
4. T. Oshima, C. Wada, Y. Kawagoe, T. Ara, M. Maeda, Y. Masuda, S. Hiraga and H. Mori, *Mol Microbiol*, 2002, 45, 673-695.
5. F. Barras and M. G. Marinus, *Trends Genet*, 1989, 5, 139-143.
6. E. Boye and A. Lobner-Olesen, *Cell*, 1990, 62, 981-989.
7. D. W. Russell and N. D. Zinder, *Cell*, 1987, 50, 1071-1079.
8. M. G. Marinus, A. Poteete and J. A. Arraj, *Gene*, 1984, 28, 123-125.
9. S. Hattman, C. Kenny, L. Berger and K. Pratt, *J Bacteriol*, 1978, 135, 1156-1157.
10. E. E. Capowski, J. M. Wells, G. S. Harrison and K. M. Karrer, *Mol Cell Biol*, 1989, 9, 2598-2605.
11. S. Hattman, *Biochemistry. Biokhimiia*, 2005, 70, 550-558.
12. C. W. Achwal, C. A. Iyer and H. S. Chandra, *FEBS Lett*, 1983, 158, 353-358.
13. Y. Fu, G. Z. Luo, K. Chen, X. Deng, M. Yu, D. Han, Z. Hao, J. Liu, X. Lu, L. C. Dore, X. Weng, Q. Ji, L. Mets and C. He, *Cell*, 2015, 161, 879-892.
14. G. Zhang, H. Huang, D. Liu, Y. Cheng, X. Liu, W. Zhang, R. Yin, D. Zhang, P. Zhang, J. Liu, C. Li, B. Liu, Y. Luo, Y. Zhu, N. Zhang, S. He, C. He, H. Wang and D. Chen, *Cell*, 2015, 161, 893-906.
15. E. L. Greer, M. A. Blanco, L. Gu, E. Sendinc, J. Liu, D. Aristizabal-Corrales, C. H. Hsu, L. Aravind, C. He and Y. Shi, *Cell*, 2015, 161, 868-878.
16. G. Egger, G. Liang, A. Aparicio and P. A. Jones, *Nature*, 2004, 429, 457-463.
17. B. F. Yuan, *Adv Clin Chem*, 2014, 67, 151-187.
18. Y. Tang, X. D. Gao, Y. Wang, B. F. Yuan and Y. Q. Feng, *Anal Chem*, 2012, 84, 7249-7255.
19. B. F. Yuan and Y. Q. Feng, *TrAC-Trend Anal Chem*, 2014, 54, 24-35.
20. A. Rottach, H. Leonhardt and F. Spada, *J Cell Biochem*, 2009, 108, 43-51.
21. P. D. Lawley, A. R. Crathorn, S. A. Shah and B. A. Smith, *Biochem J*, 1972, 128, 133-138.
22. B. F. Vanyushin, S. G. Tkacheva and A. N. Belozersky, *Nature*, 1970, 225, 948-949.
23. A. M. Krais, M. G. Cornelius and H. H. Schmeiser, *Electrophoresis*, 2010, 31, 3548-3551.
24. M. Munzel, D. Globisch and T. Carell, *Angew Chem Int Ed Engl*, 2011, 50, 6460-6468.
25. M. R. Branco, G. Ficz and W. Reik, *Nat Rev Genet*, 2012, 13, 7-13.

26. G. Jia, Y. Fu and C. He, *Trends Genet*, 2013, 29, 108-115.
27. C. M. Wei, A. Gershowitz and B. Moss, *Cell*, 1975, 4, 379-386.
28. R. Desrosiers, K. Friderici and F. Rottman, *Proc Natl Acad Sci U S A*, 1974, 71, 3971-3975.
29. K. D. Meyer, Y. Saletore, P. Zumbo, O. Elemento, C. E. Mason and S. R. Jaffrey, *Cell*, 2012, 149, 1635-1646.
30. D. Dominissini, S. Moshitch-Moshkovitz, S. Schwartz, M. Salmon-Divon, L. Ungar, S. Osenberg, K. Cesarkas, J. Jacob-Hirsch, N. Amariglio, M. Kupiec, R. Sorek and G. Rechavi, *Nature*, 2012, 485, 201-206.
31. J. M. Fustin, M. Doi, Y. Yamaguchi, H. Hida, S. Nishimura, M. Yoshida, T. Isagawa, M. S. Morioka, H. Kakeya, I. Manabe and H. Okamura, *Cell*, 2013, 155, 793-806.
32. S. Schwartz, S. D. Agarwala, M. R. Mumbach, M. Jovanovic, P. Mertins, A. Shishkin, Y. Tabach, T. S. Mikkelsen, R. Satija, G. Ruvkun, S. A. Carr, E. S. Lander, G. R. Fink and A. Regev, *Cell*, 2013, 155, 1409-1421.
33. Y. Fu, D. Dominissini, G. Rechavi and C. He, *Nat Rev Genet*, 2014, 15, 293-306.
34. X. Wang, Z. Lu, A. Gomez, G. C. Hon, Y. Yue, D. Han, Y. Fu, M. Parisien, Q. Dai, G. Jia, B. Ren, T. Pan and C. He, *Nature*, 2014, 505, 117-120.
35. F. Shen, W. Huang, J. T. Huang, J. Xiong, Y. Yang, K. Wu, G. F. Jia, J. Chen, Y. Q. Feng, B. F. Yuan and S. M. Liu, *J Clin Endocrinol Metab*, 2015, 100, E148-154.
36. Y. Tang, J. M. Chu, W. Huang, J. Xiong, X. W. Xing, X. Zhou, Y. Q. Feng and B. F. Yuan, *Anal Chem*, 2013, 85, 6129-6135.
37. X. W. Xing, Y. L. Liu, M. Vargas, Y. Wang, Y. Q. Feng, X. Zhou and B. F. Yuan, *PLoS One*, 2013, 8, e72993.
38. Y. Tang, J. Xiong, H. P. Jiang, S. J. Zheng, Y. Q. Feng and B. F. Yuan, *Anal Chem*, 2014, 86, 7764-7772.
39. G. Jia, Y. Fu, X. Zhao, Q. Dai, G. Zheng, Y. Yang, C. Yi, T. Lindahl, T. Pan, Y. G. Yang and C. He, *Nat Chem Biol*, 2011, 7, 885-887.
40. M. L. Chen, F. Shen, W. Huang, J. H. Qi, Y. Wang, Y. Q. Feng, S. M. Liu and B. F. Yuan, *Clin Chem*, 2013, 59, 824-832.
41. X. T. Peng, B. F. Yuan and Y. Q. Feng, *J Sep Sci*, 34, 3123-3130.
42. P. Liu, X.-H. Yang, Q. Wang, J. Huang, J.-B. Liu, Y. Zhu, L.-L. He and K.-M. Wang, *Chinese Chem Lett*, 2014, 25, 1047-1051.
43. X. W. Xing, F. Tang, J. Wu, J. M. Chu, Y. Q. Feng, X. Zhou and B. F. Yuan, *Anal Chem*, 2014, 86, 11269-11274.

RSC Advances

ARTICLE

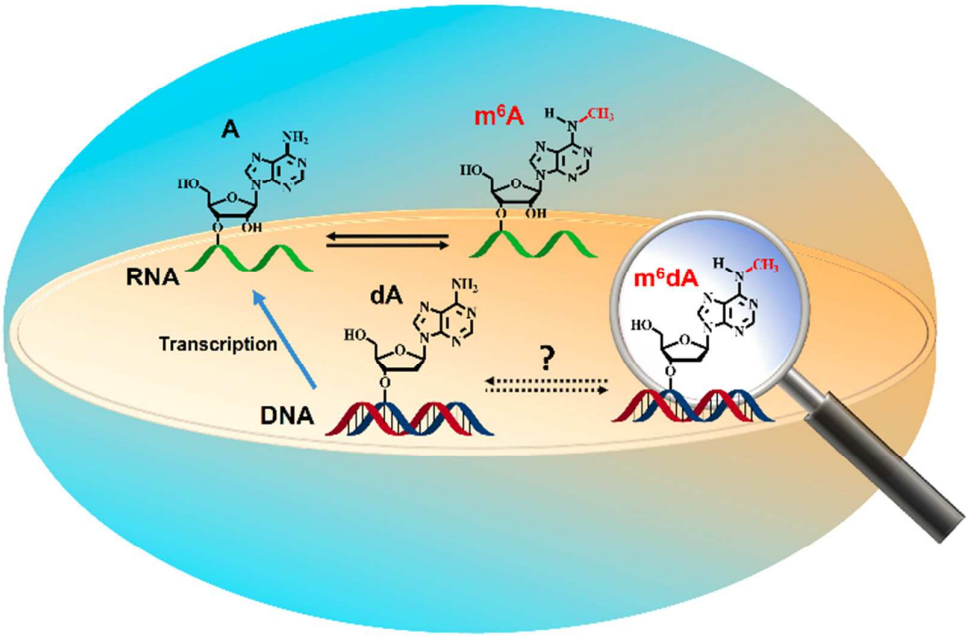

Table of content: Determination of DNA Adenine Methylation in Genomes of Mammals and Plants